Molecular-beam epitaxy of InSb/GaSb quantum dots

N. Deguffroy, V. Tasco,[a] A. N. Baranov, and E. Tournié[b]
Institut d'Electronique du Sud (IES), CC 067, Université Montpellier 2, CNRS, UMR 5214, Place Eugène Bataillon, F-34095 Montpellier Cedex 5, France

B. Satpati and A. Trampert
Paul-Drude-Institut für Festkörperelektronik, Hausvogteiplatz 5-7, D-10117 Berlin, Germany

M. S. Dunaevskii and A. Titkov
Ioffe-Physico-Technical Institute, 194021 St. Petersburg, Russia

M. Ramonda
Laboratoire de Microscopie en Champ Proche, CC 082, Université Montpellier 2, Place Eugène Bataillon, F-34095 Montpellier, Cedex 5, France

(Received 20 March 2007; accepted 7 May 2007; published online 25 June 2007)

We have investigated the molecular-beam epitaxy (MBE) of InSb nanostructures on (100) GaSb substrates. We show that MBE leads to a low density ($\sim 1-3\times 10^9$ cm^{-2}) of large islands even when varying the growth conditions on a wide range (substrate temperature $\sim 370-450$ °C, growth rate $\sim 0.3-1.2$ ML/s). Plastic relaxation takes place from the onset of island formation, regardless of the amount of InSb deposited after the two-dimensional to three-dimensional transition. These results show that In adatoms have a very long diffusion length on a Sb-terminated surface and that the energy for dislocation generation in InSb is low. This can be attributed to the low enthalpy of formation and low melting point of InSb. To circumvent this problem we have developed a MBE growth procedure based on the deposition of an amorphous InSb layer at low temperature followed by an annealing step to allow for reorganization to take place. This dramatic change of the growth conditions leads to the formation of small InSb quantum dots with a density in excess of 7×10^{10} cm^{-2}. Uncapped quantum dots, however, are relaxed. In contrast, buried quantum dots are fully strained and emit near 3.5 μm at room temperature. Our results show that although formerly similar the InSb/GaSb materials system behaves completely differently from the InAs/GaAs case study system. © *2007 American Institute of Physics*. [DOI: 10.1063/1.2748872]

I. INTRODUCTION

The past decade has seen a tremendous development in the field of semiconductor quantum dots (QDs) which has been driven, on the one hand, by their unique physical properties and, on the other hand, by their potential impact in the realm of electronic and photonic devices.[1] Most work in this field has been carried out on the seminal Si/Ge and $Ga_{1-x}In_xAs/GaAs$ materials system grown by molecular-beam epitaxy (MBE). This last case is particularly well documented.[2] It is now established that MBE growth proceeds two-dimensionally (2D) for a strain below ~2% ($x=0.3$) while there is a 2D to three-dimensional (3D) transition leading to the formation of QDs for larger strain (Stranski–Krastanov growth). In the extreme case of InAs on GaAs the transition occurs near 1.5 ML.[2] A similar behavior to this prototypical case study is often assumed for any III–V semiconductor system, even when they have been only barely studied. A particularly interesting system in this respect is InSb/GaSb. Indeed, with a lattice mismatch of 6.3% it is formally very similar to InAs/GaAs (7.3% lattice mismatch), the main difference being the group-V element (Sb vs As). Given the narrow-band gap of antimonides compounds, InSb QDs are appealing candidates to the fabrication of the high performance midinfrared nanophotonic devices which are needed for various applications such as gas analysis, free-space optics, or countermeasures.[3]

The first investigations of the MBE growth of InSb on GaSb have shown that InSb obeys the Stranski–Krastanow growth mode, with a 2D-3D transition occurring around 1.7 ML under typical conditions (growth temperature $\sim 400-450$ °C, rate $\sim 0.5-1$ ML/s, Sb/In flux ratio >2).[4] Subsequently, one group reported the formation of a high density of small coherent islands right at the growth-mode transition (1.7 ML) during MBE of InSb on GaSb.[5,6] It is not clear, however, whether at this stage these nanostructures are real-3D dash-like InSb islands[5] or rather monolayer-high 2D InSb islands.[6] Large, relaxed islands formed for any thicker InSb layer.[5,6] All other studies have confirmed the initial results and have shown that a low density of large InSb islands are formed whatever the growth technique, MBE,[7] or metal-organic vapor phase epitaxy.[8–10] This behavior apparently differs from the InAs/GaAs case. Indeed, we have recently demonstrated that a special MBE growth procedure allows the formation of high density InSb QDs on GaSb.[11,12] In this work we present a detailed study of the MBE growth and properties of InSb/GaSb heterostructures which shows that this system differs totally from InAs/GaAs.

[a]Present address: National Nanotechnology Laboratory, CNR-INFM, Lecce, Italy.
[b]Electronic mail: etournie@univ-montp2.fr

 © 2007 American Institute of Physics

Downloaded 16 Jul 2007 to 62.141.165.15. Redistribution subject to AIP license or copyright, see http://jap.aip.org/jap/copyright.jsp

II. EXPERIMENTS

The samples have been grown on (100)-oriented GaSb wafers by solid-source MBE in a system equipped with As- and Sb-valved cracker cells. *In situ* reflection high energy electron diffraction (RHEED) has been used to monitor the growth. The flux, expressed in ML/s, of all—group-III as well as group-V—elements have been determined by RHEED intensity oscillations measurements. All layers were grown with a Sb/III ratio of ~2. The GaSb deoxydation occurs at a pyrometer reading of ~550 °C in our system. Most InSb layers, grown under the various conditions described later, have been inserted in the center of a 300 nm-thick GaSb barrier itself confined by lattice-matched AlGaAsSb layers. For a series of samples positive-intrinsic-negative (*p-i-n*) structures were grown to investigate electroluminescence (EL) properties. For another series, the InSb layers were left uncapped. In that case the substrate heating system was switched off immediately after InSb growth or QDs formation.

Uncapped samples have been studied by atomic force microscopy (AFM) and transmission electron microscopy (TEM) to assess their structural properties. Complete heterostructures have been characterized by TEM, and photoluminescence (PL) or EL spectroscopies at 90 and 300 K. A semiconductor diode laser operating at 650 nm was used for optical pumping. The PL spectra were recorded using a Fourier-transform infrared spectrometer equipped with a liquid-nitrogen cooled InSb detector.

Detailed AFM investigations have been performed on SOLVER P-47 device (NT-MDT production, Zelenograd, Russia) in which model a scanning of the sample surface is performed via scanning of the sample beneath the AFM probe. That scanning arrangement gives a higher lateral resolution compared to many devices in which the sample is fixed and scanning is performed via an AFM probe movement along the sample surface. AFM topography studies were performed in semicontact mode with NT-MDT AFM probes NSG11 and NSC05 (whisker type) with the tip apex radius typically smaller then 10 nm. These experimental arrangement permits to achieve a nanometer spatial resolution. A statistical analysis using specially developed software was applied to obtain the average height and radius values for all InSb QDs ensemble.

TEM has been performed by PDI Berlin. The TEM analysis was carried out in a Jeol JEM-3010UHR microscope operating at 300 kV. The cross-sectional TEM samples were prepared by standard techniques using mechanical grinding and dimpling. Finally, the samples were sputtered until electron transparency by an argon ion beam using 2.5–3.0 keV energy in order to avoid strong sputter damage. During all processing steps, a minimum mechanical load was applied to the samples to minimize the external stresses.

III. GROWTH OF INSB ON GASB UNDER USUAL MBE CONDITIONS

A. RHEED and AFM observations

We first investigated the MBE growth of InSb directly onto GaSb for substrate temperatures around 450 °C and growth rates around 0.3 ML/s. We observe that under these conditions InSb obeys the Stranski–Krastanow mode with a 2D-3D transition occurring around 1.7 ML, depending on the precise conditions. We show in Fig. 1 typical AFM images for 2.4 ML InSb deposited at 450 °C and 0.33 ML/s. They confirm the presence of low density islands ($\sim 2 \times 10^9$ cm^{-2}). In addition, their typical main axis length and height are ~50 and 8 nm, respectively, with a high dispersion. These observations agree well with previous reports.[4,6–8]

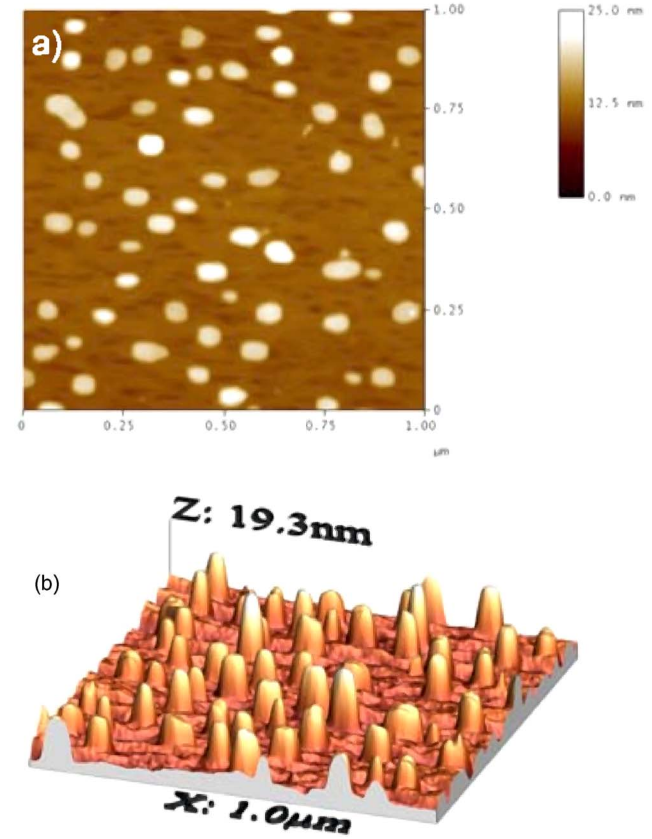

FIG. 1. (a) Top-view AFM image and (b) 3D-view AFM image of 2.4 ML InSb deposited on GaSb at 450 °C and 0.33 ML/s.

B. Microstructure of InSb islands

We have investigated such nanostructures embedded within a *p-i-n* structure by TEM (Fig. 2). Several interesting features are to be noticed. The size of the buried islands determined by TEM is similar to the size of uncapped islands measured by AFM. In addition, all islands—even though they are buried—are highly defective containing misfit dislocations at the interface and dislocation loops around the islands (inset in Fig. 2). This shows that the self-organization of the InSb layer takes place on an extremely short time scale with an early onset of plastic relaxation accompanied by a low activation barrier for dislocation generation. The analysis of the lattice parameter reveals that it corresponds—within the error bar—to the parameter of fully relaxed, pure InSb. Finally, in spite of the high defect density within the QDs, only part of them gives rise to defects propagating through the upper layers.

Downloaded 16 Jul 2007 to 62.141.165.15. Redistribution subject to AIP license or copyright, see http://jap.aip.org/jap/copyright.jsp

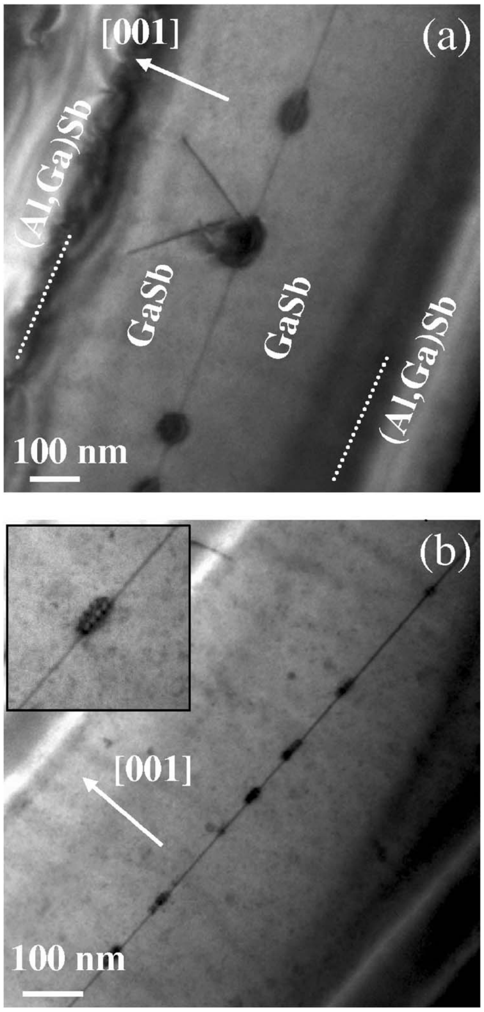

FIG. 2. (a) TEM images taken from 2.4 ML inSb inserted in a *p-i-n* structure and (b) details of the QDs microstructure. The inset shows dislocation loops in an individual InSb QD.

C. Influence of growth kinetics

We have then varied the growth parameters in a wide range. The substrate temperature has been changed between 370 and 450 °C, the InSb growth rate between 0.3 and 1.2 ML/s, the Sb/In flux ratio between 1 and 5, and the InSb amount from 1.8 to 2.5 ML. We have also introduced 2–10 nm-thick AlGaSb or AlGaAsSb layers between the GaSb and InSb layers. The surface of Al-containing alloys being less perfect than the GaSb surface they should favor heterogeneous nucleation and promote the formation of a high density of QDs. However, although these variations cover a wide range of growth conditions, the properties of the QDs populations were only marginally affected. A striking point is that all islands are fully relaxed from the onset of QDs formation whatever the amount of InSb which has been deposited after the 2D-3D transition. Needless to say, such defective nanostructures are not compatible with the development of any device. Finally, we note also that these large islands can barely be considered as QDs in the sense of quantum mechanics.

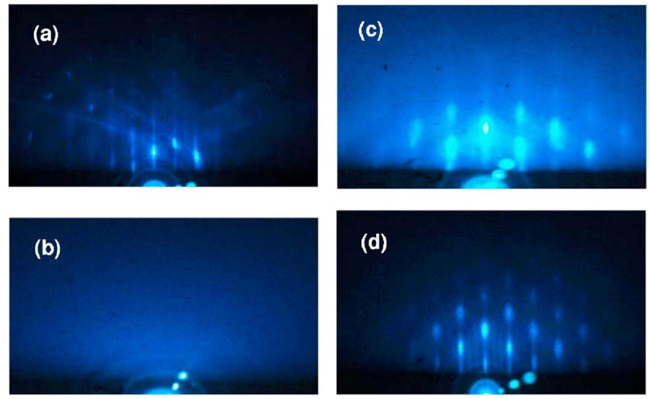

FIG. 3. RHEED patterns taken (a) from the GaSb layer at 300 °C ([110] azimuth), (b) after deposition of 2.5 ML InSb at 300 °C ([1–10] azimuth), (c) at 360 °C during the temperature ramp-up ([1–10] azimuth), and (d) after 20 s annealing at 390 °C ([1–10] azimuth).

IV. A MODIFIED-MBE ROUTE FOR THE GROWTH OF INSB QDS ON GASB

The results shown earlier indicate that an alternative route is needed to overcome these limitations and to obtain dot densities and properties suitable for device applications.

A. Growth procedure—RHEED and AFM observations

A further particularity of Sb with respect to other usual group-V elements is that it condensates easily on a GaSb surface when decreasing the substrate temperature. In our system, this condensation occurs at a pyrometer reading of ~380 °C for a Sb-limited growth rate of 1.5 ML/s. We have thus developed a special growth procedure which takes profit of this property. Indeed, both low temperature and solid-Sb are used to drastically shorten the In-migration length which is mostly responsible for the quick formation of large and plastically relaxed islands.

After completion of the GaSb buffer layer we reduce the substrate temperature down to ~250–300 °C. The Sb shutter is closed at around 400 °C. The RHEED pattern then indicates an evolution from a (1×3) to a (2×5) reconstruction at ~430 °C.[13] This reconstruction remains unchanged and bright down to 250–300 °C [Fig. 3(a)]. AFM pictures taken at the completion of the buffer layer reveal a perfect surface ordering with monolayer-high terraces [Fig. 4(a)]. A few MLs of InSb are then deposited. The RHEED pattern turns very faint or even totally blurry, which is characteristic for an amorphous surface [Fig. 3(b)]. Indeed, at this temperature an amorphous or polycrystalline InSb film is expected. At this stage AFM [Fig. 4(b)] reveals a uniform surface with a root mean square roughness of about 6 ML. Immediately after InSb deposition, the substrate temperature is increased up to the Sb-desorption value (390 °C) where an annealing is performed during ~20–50 s. The RHEED pattern evolves toward a spotty-like pattern indicating the formation of well developed QDs [Figs. 3(c) and 3(d)]. Figure 4(c) shows the AFM image taken from 2.5 MLs of InSb deposited according to this procedure.

Downloaded 16 Jul 2007 to 62.141.165.15. Redistribution subject to AIP license or copyright, see http://jap.aip.org/jap/copyright.jsp

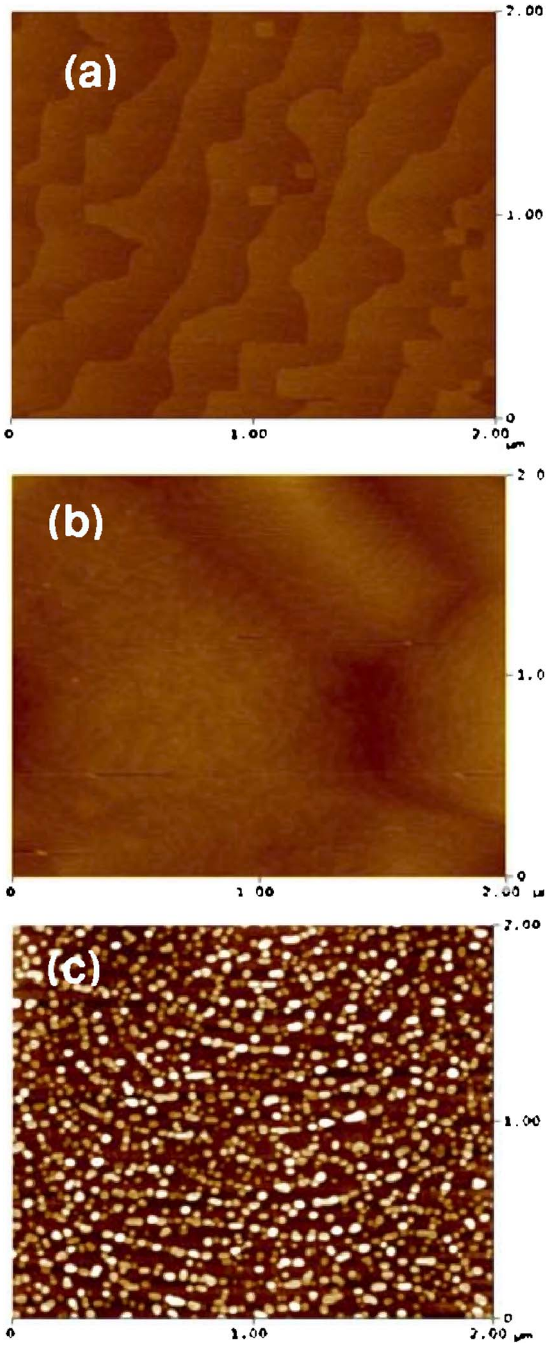

FIG. 4. AFM images taken (a) from the GaSb buffer layer, (b) after deposition of 2.5 ML InSb at 300 °C, and (c) after 20 s annealing at 390 °C.

The uniform surface observed after the InSb deposition at low temperature has been replaced by well defined nanostructures after the annealing step. We obtain a dot density as high as 7.4×10^{10} cm^{-2}, i.e., at least one order of magnitude higher than ever reported for similar InSb amounts. The QDs average sizes are 13 ± 3 nm for the radius and 1.7 ± 0.5 nm for the height. Therefore, this two-step growth technique enables a noticeable improvement of the QD population with respect to any other reported conditions besides the results obtained right at the transition thickness, 1.7 ML InSb.[5,6]

We have then investigated the microstructure of InSb QDs grown under this alternative growth procedure.

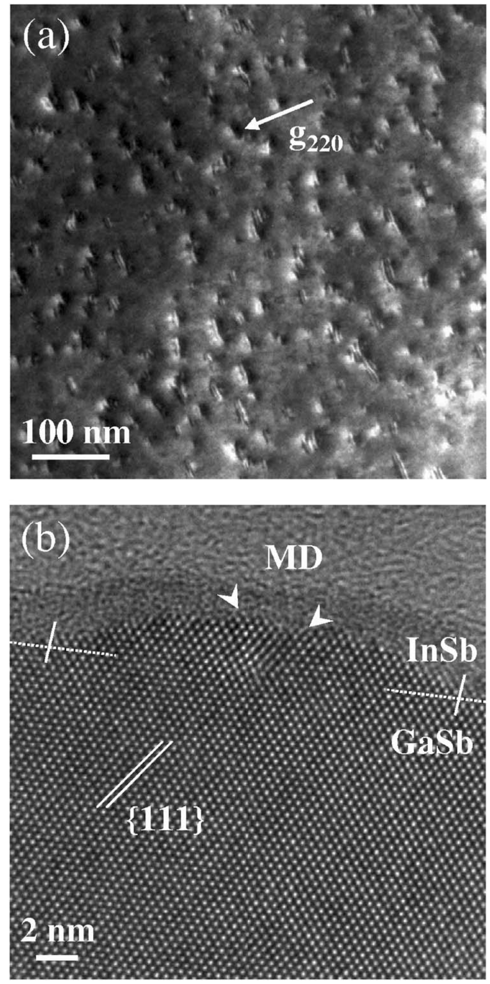

FIG. 5. (a) Plan-view (220) dark-field TEM image of partially strain relieved InSb islands grown on GaSb (001) at low temperature and (b) high resolution TEM (HRTEM) image showing pure-edge type misfit dislocation at the interface.

B. Microstructure of uncapped InSb QDs

First, uncapped InSb islands were structurally investigated by conventional and high-resolution TEM. Figure 5(a) displays a plan-view dark-field TEM image of an uncapped InSb layer of nominal 2.5 ML thickness grown at 300 °C followed by subsequent annealing. This image reveals the presence of small and flat InSb QDs with a monomodal size distribution and an average diameter of about 20 nm. These data agree well with the AFM images described previously (Fig. 4). However, based on the strain sensitive imaging condition (with $\mathbf{g}_{220}$ reflection), we find that most of the islands are plastically relaxed by the introduction of misfit dislocations at the interface. The cross-sectional high-resolution TEM image displayed in Fig. 5(b) demonstrates the presence of such a misfit dislocation in the center of the island being of pure-edge type with Burger vector $\mathbf{b} = 1/2[1\bar{1}0]$, which is most efficient in strain relief. Because of the sessile character of the dislocation it is assumed that its formation proceeds during the annealing process, when the InSb islands are formed on the free surface.

The nucleation of InSb on GaSb is characterized by the formation of tiny, flat islands, at the beginning which are

Downloaded 16 Jul 2007 to 62.141.165.15. Redistribution subject to AIP license or copyright, see http://jap.aip.org/jap/copyright.jsp

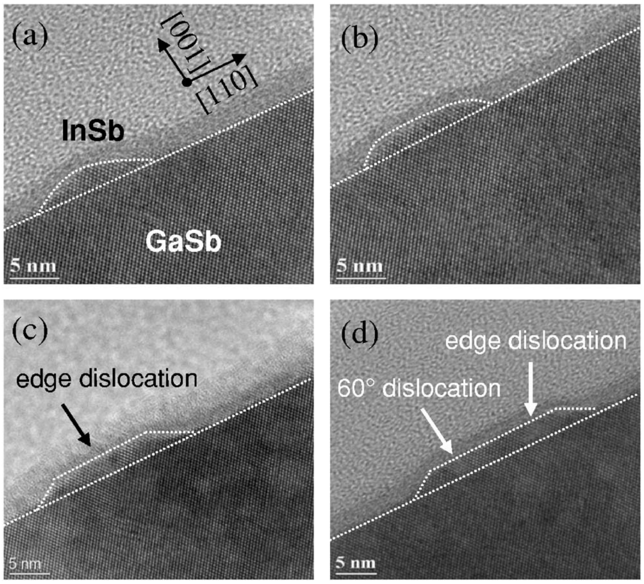

FIG. 6. (a)–(d) Experimental cross-sectional HRTEM images showing size and shape evolution of QDs.

completely coherently strained to the substrate. These small QDs have a round and lens-shaped form [Figs. 6(a) and 6(b)]. With further annealing and/or deposition the coherent islands grow in all directions until a critical dimension is achieved and plastic relaxation starts with the formation of misfit dislocations [Fig. 6(c)]. This process is driven by the minimization of the strain and surface/interface energies. The larger and relaxed QDs always have flat surfaces and {111} sidefacets [indicated by white dotted lines in Fig. 6(d)]. The evolution of the InSb QDs is schematically summarized in Fig. 7. It is remarkable that partly relaxed islands tend to grow faster in the lateral direction (the height remains almost constant) and, simultaneously, establish energetically favorable facets. At the same time, with increasing size, the strain relaxation proceeds by forming a more and more dense array of misfit dislocations. Additionally, this TEM analysis (Fig. 7) determines the critical QDs size of about 12 nm for the onset of plastic relaxation. Note that AFM gives an average value for the diameter of 13 ± 3 nm (cf. Sec. IV A). Most uncapped InSb QDs are thus plastically relaxed.

C. Microstructure of buried InSb QDs

Compared to the uncapped island case, a completely different situation is observed when the InSb QD population is frozen by growing a GaSb layer immediately after QDs formation. Figure 8(a) shows a (002) bright-field TEM image of such a buried QD sample. It demonstrates the existence of a wetting layer with a high density of tiny QDs as a result of the strong contrast variations along the InSb layer compared to the homogeneous contrast of the adjoining GaSb. Note that the complete structure is free of any extended defects. No threading dislocations are observed indicating that there is no plastic relaxation process involved. By tilting the sample around the [110] axis, the interface becomes inclined to the electron beam which enables the observation of isolated InSb QDs. Applying the $\mathbf{g}=220$ diffraction condition, the strain field of the QDs is detected in this direction reveal-

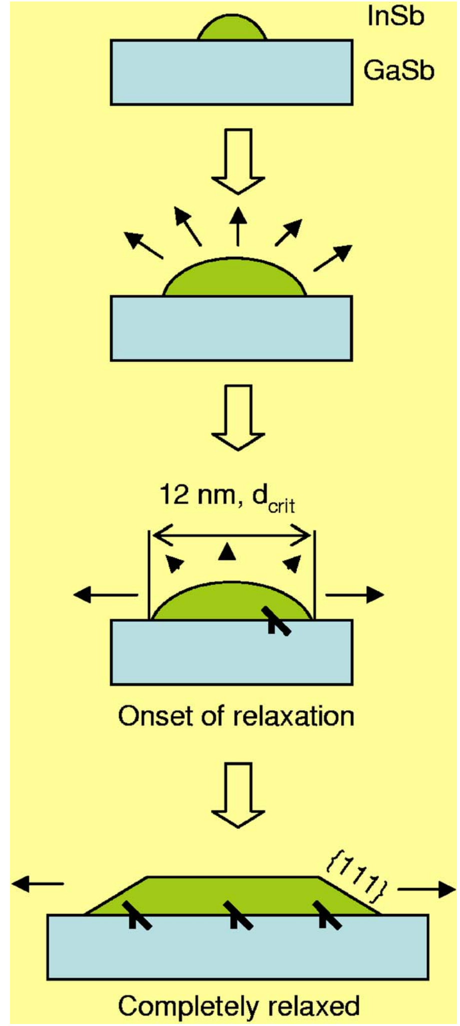

FIG. 7. Schematic of the QDs evolution for InSb QDs grown at low temperature. We observe a critical diameter d_{crit} ($\approx$12 nm) beyond which islands starts relaxing. These relaxed islands have {111} sidefacets.

ing an average size of about 10 nm. In detail, the lattice strain around the InSb QDs appears as lobes of dark contrast (low intensity) with lines-of-no-contrast perpendicular to **g** [the so called coffee bean contrast, more evident in the inset of Fig. 8(b)]. This particular strain effect corresponds to fully strained InSb QDs with a lens shape.[14]

D. Electronic properties

We have performed preliminary investigations of the luminescence properties of buried InSb QDs grown under the alternative MBE conditions. We show in Fig. 9 PL spectra taken at 90 K under different excitation densities (from 0.4 to 10 $\mathrm{W/cm^2}$) from a sample containing one plan of InSb QDs obtained by depositing 3 ML InSb. In the high energy region, two peaks are detected at 0.79 and at 0.72_5 eV. We assign them to GaSb and its native defects[15] and to the wetting layer.[6] The other two transitions at 0.367 eV (i.e., ~3.4 μm) and at ~0.5 eV come from QDs-related transitions, as confirmed by experiments which show that these lines disappear upon etching the sample down to the buffer layer. The lowest energy peak is attributed to the system ground state transition, whereas the line at 0.5 eV is temptatively attributed to

Downloaded 16 Jul 2007 to 62.141.165.15. Redistribution subject to AIP license or copyright, see http://jap.aip.org/jap/copyright.jsp

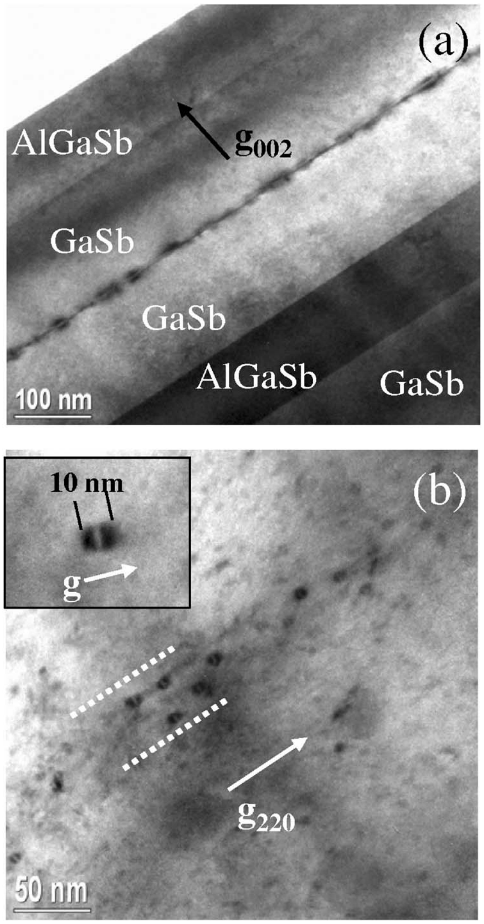

FIG. 8. TEM cross-sectional images of 3 ML InSb QDs grown with the two step technique. Cross-sectional 002 bright–field (a) TEM of buried InSb QDs and projectional view (b) of tilted QDs layer (**g**=220) in bright-field mode to visualize the isolated QDs. The inset in (b) is a zoom on two InSb QDs showing the characteristic coffee beam contrast of fully strained nanostructures.

the system first excited state. In addition, PL has been observed up to room temperature with a quenching factor as low as 4. The emission then peaks at 0.326 eV, i.e., ~3.8 μm.[12] Electroluminescence analysis was also performed on the same type of active region inserted in a dedicated *p-i-n* junction, with doped AlGaAsSb cladding layers. Figure 10 shows the EL spectra at 90 K for different electrical injection conditions. Again, an emission centered at 0.367 eV is observed with efficiency and linewidth increasing with the average driving current. Both PL and EL spectra thus give a ground state transition at 0.367 eV at 90 K. This energy is lower than previously reported[5,6,16] and cannot be simply explained by considering a type-I transition in InSb/GaSb QDs. This may be explained by taking into account the tensile strain in the GaSb matrix around the QDs. This strain locally lowers the GaSb conduction band thus localizing the electrons and resulting in a type-II alignment with a low transition energy.[17] Elucidation of the precise band structure of these QDs is a very complex matter which is much beyond the scope of this work. Detailed calculations coupled to experiments are indeed in progress to clarify the situation.[17]

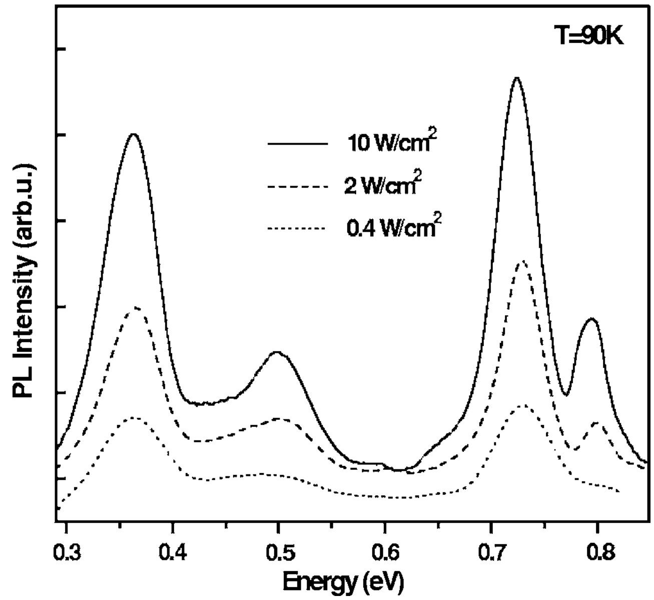

FIG. 9. Photoluminescence spectra taken from a single InSb QDs plan (a) under various excitation power at 90 K.

V. DISCUSSION–CONCLUSION

The results obtained for the large number of experiments described earlier can only be explained if one assumes that In has a long diffusion length on a Sb-terminated surface under a wide range of MBE growth conditions. In addition, the usual parameters are not efficient enough to alter the growth kinetics of the system. In fact, both In and Sb elements have in common that they exhibit the largest atomic *radii* among the usual group-III and group-V elements. In addition, the enthalpies of formation of In-V and III-Sb compounds are the lowest among all III–V compounds.[18] The cohesive energy of InSb is thus the lowest among all III–V compounds. Consequently, In adatoms falling onto a Sb-terminated surface have a long residence time before being incorporated. They can move over long distances and form large clusters. We note that these findings are in agreement with the par-

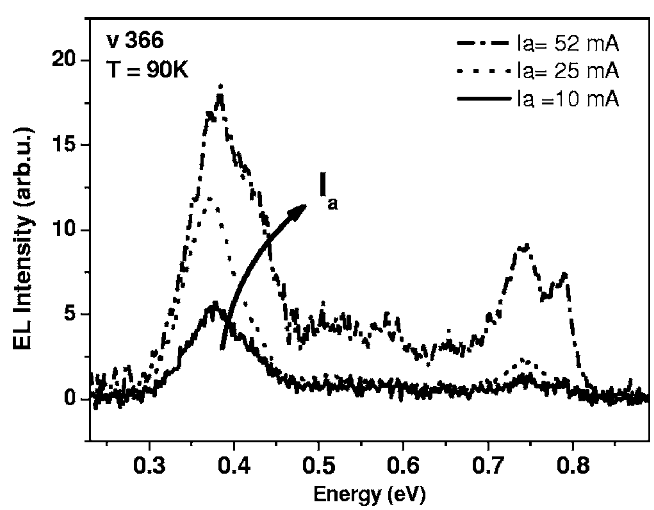

FIG. 10. Electroluminescence spectra taken at 90 K from a single InSb QDs plan embedded in a *p-i-n* junction under various pulsed conditions corresponding to the average drive-currents Ia.

Downloaded 16 Jul 2007 to 62.141.165.15. Redistribution subject to AIP license or copyright, see http://jap.aip.org/jap/copyright.jsp

ticular role that both In and Sb play during epitaxy of a variety of lattice-mismatch III–V semiconductor heterostructures.[19] Indeed, they behave as surfactants and tend to promote 2D rather than 3D growth.

Our alternative route, however, has proved efficient to obtain true, fully strained InSb QDs on GaSb. The results are interpreted as follows. At a temperature as low as 300 °C, not only the In-migration length is naturally reduced, but also Sb-solid clusters are formed which further suppress In migration. The annealing step allows the evaporation of the excess Sb. The InSb film crystallizes and evolves toward its lowest energy state, i.e., formation of well developed QDs. It is noticeable that each parameter involved in this procedure (amount of deposited material, V/III ratio, heating rate, and annealing time) has its own effect on the final result. For example, a too long annealing step or an annealing step at too high a temperature lead to large, relaxed QDs which are similar to those grown directly under regular MBE conditions (cf. Sec. III).

The different microstructures observed between uncapped and buried InSb QDs (cf. Secs. IV B and IV C) are also related to the high diffusion length of adatoms. Indeed, even when turning the substrate oven off, it takes several minutes to cool the uncapped QDs samples from the annealing temperature ($\sim 390\ ^\circ\mathrm{C}$) down to the temperature at which the situation is frozen out. During this stage Ostwald ripening starts taking place which results in larger QDs which are relaxed. This is also in agreement with the impact of the duration of the annealing step mentioned earlier. In contrast, overgrowing the QDs at the end of the annealing step freezes immediately the situation. Defect-free QDs are then obtained.

These results show that albeit apparently similar the InSb/GaSb system differs totally from its InAs/GaAs counterpart from the point of view of QDs formation as well as from the point of view of their structural properties. Indeed in the later case small, coherent islands form naturally upon MBE growth[2] while in the former it has been necessary to develop a specific growth procedure to achieve InSb QDs. Antimonide-based QDs thus open a new route into the realm of semiconductor nanostructures.

ACKNOWLEDGMENT

Part of this work has been sponsored by the European Commission (Project No. FP6-017383, DOMINO).

[1] See, e.g., *Nano-Optoelectronics*, edited by M. Grundmann (Springer, Berlin, 2002).
[2] See, e.g., *Epitaxy of Nanostructures*, edited by V. A. Schuchkin, N. N. Ledentsov, and D. Bimberg (Springer, Berlin, 2004).
[3] See, e.g., *Mid-Infrared Semiconductor Optoelectronics*, edited by A. Krier (Springer, Berlin, 2006).
[4] N. Bertru, O. Brandt, M. Wassermeier, and K. Ploog, Appl. Phys. Lett. **68**, 31 (1996).
[5] A. F. Tsatsul'nikov, S. V. Ivanov, P. S. Kop'ev, A. K. Kryganovskii, N. N. Ledenstov, M. V. Maximov, B. Ya. Mel'tser, P. V. Nekludov, A. A. Suvurova, A. N. Tiktov, B. V. Volovik, M. Grundman, D. Bimberg, and Zh. I. Alferov, J. Electron. Mater. **27**, 414 (1998).
[6] A. F. Tsatsul'nikov, S. V. Ivanov, P. S. Kop'ev, I. L. Krestnikov, A. K. Kryganovskii, N. N. Ledenstov, M. V. Maximov, B. Ya. Mel'tser, P. V. Nekludov, A. A. Suvurova, A. N. Tiktov, B. V. Volovik, M. Grundman, D. Bimberg, and Zh. I. Alferov, Microelectron. Eng. **43–44**, 85 (1998).
[7] N. Deguffroy, M. Ramonda, A. N. Baranov, and E. Tournié, Inst. Phys. Conf. Ser. **187**, 89 (2006).
[8] E. Alphandéry, R. J. Nicholas, N. J. Mason, B. Zhang, P. Möck, and G. R. Booker, Appl. Phys. Lett. **74**, 2041 (1999).
[9] P. Möck, G. R. Booker, N. J. Mason, R. J. Nicholas, E. Alphandéry, T. Topuria, and N. D. Browning, Mater. Sci. Eng. B **80**, 112 (2001).
[10] S. Shusterman, Y. Paltiel, A. Sher, V. Ezersky, and Y. Rosenwaks, J. Cryst. Growth **291**, 363 (2006).
[11] V. Tasco, N. Deguffroy, A. N. Baranov, E. Tournié, B. Satpati, and A. Trampert, Phys. Status Solidi B **243**, 3959 (2006).
[12] V. Tasco, N. Deguffroy, A. N. Baranov, E. Tournié, B. Satpati, A. Trampert, M. Dunaevski, and A. Tiktov, Appl. Phys. Lett. **89**, 263118 (2006).
[13] A. S. Bracker, M. J. Yang, B. R. Bennett, J. C. Culbertson, and W. J. Moore, J. Cryst. Growth **220**, 384 (2000).
[14] D. B. Williams and C. B. Carter, *Transmission Electron Microscopy: A Textbook in Material Science* (Plenum, New York, 1996), Part III, p. 417.
[15] P.S. Dutta, H. L. Bhat, and V. Kumar, J. Appl. Phys. **81**, 5821 (1997).
[16] E. Alphandéry, R. J. Nicholas, N. J. Mason, S. G. Lyapin, and P. C. Klipstein, Phys. Rev. B **65**, 115322 (2002).
[17] S. I. Rybchenko, R. E. Gupta, I. E. Itskevich, and S. K. Haywood (private communication).
[18] See, e.g., V. P. Vasil'ev and J. P. Gachon, Inorg. Mater. **42**, 1176 (2006).
[19] E. Tournié and A. Trampert, Phys. Status Solidi B 244, in press.

Downloaded 16 Jul 2007 to 62.141.165.15. Redistribution subject to AIP license or copyright, see http://jap.aip.org/jap/copyright.jsp